Eur. Phys. J. D **4**, 199–205 (1998)

THE EUROPEAN PHYSICAL JOURNAL D

Reaction dynamics of Cl + O_3 → ClO + O_2

S. Baumgärtel, R.F. Delmdahl, K.-H. Gericke[a], and A. Tribukait[b]

Technische Universität Braunschweig, Institut für Physikalische und Theoretische Chemie, Hans-Sommer-Strasse 10, 38106 Braunschweig, Germany

Received: 27 February 1998 / Revised: 1st April 1998 / Accepted: 15 April 1998

Abstract. Applying the two photon laser induced fluorescence technique for nascent state resolved $ClO(X^2\Pi_\Omega,\ v,\ J)$ detection, the reaction dynamics of $Cl+O_3 \rightarrow ClO+O_2$ is investigated. The ClO product is formed in its electronic ground state $ClO(X^2\Pi_\Omega)$. A complete product state analysis in terms of vibration, rotation, spin-orbit and Λ-states indicates that nascent ClO radicals are formed in $v = 0$–6 vibrational states peaking at $v = 3$. The ClO fragment shows a moderate rotational excitation, described by a Boltzmann distribution with a temperature parameter of 1300 K ± 200 K. The spin orbit ratio of $P(^2\Pi_{3/2}):P(^2\Pi_{1/2}) = 1.5 \pm 0.3$. Most of the excess energy is released as translational energy or as internal energy of the O_2 product. By comparing our results with the trajectory studies of Farantos and Murrell, we favour a reaction mechanism, where the transition complex is planar containing an essentially linear OOCl group. In order to determine the possible influence of vibrationally excited ClO on other trace components of the atmosphere, especially the reaction $ClO(v > 0)+ O_3$, a rough estimate of the vibrational relaxation rate of ClO with the major atmospheric collision partner, N_2, has been performed. A measurement of the vibrational distribution of ClO at different N_2 pressures indicates a mean vibrational relaxation rate of $k = 2 \times 10^{-13}$ cm^3 molecule^{-1}s^{-1}.

PACS. 34.50.Lf Chemical reactions, energy disposal, and angular distribution, as studied by atomic and molecular beams – 82.20.Hf Mechanisms and product distribution – 94.10.Fa Atmospheric composition (atomic or molecular), chemical reactions and processes

1 Introduction

The importance of chlorine monoxide in atmospheric chemistry was first emphasized in 1976 [1], where the following reactions

$$Cl + O_3 \rightarrow ClO + O_2 \quad (1)$$

$$ClO + O \rightarrow Cl + O_2 \quad (2)$$

are assumed to be a catalytic cycle for removal of ozone in the stratosphere. Later, other authors discovered additional catalytic cycles of the stratospheric ozone loss mechanisms where ClO plays a central role [2–6]. In this context, there is great interest in reaction 1 and consequently a large number of investigations of the kinetics of reaction 1 has been performed [7–10]. The measurements yielded a recommended rate coefficient of $2.9 \times 10^{-11} \exp(-260/T)$ cm^3 molecule^{-1}s^{-1} in a temperature range of 205–298 K [11].

Electronically excited ClO cannot be formed in reaction 1 because the exothermicity of this reaction ($\Delta_R H = -162.6$ kJ/mol) is insufficient in order to reach the first excited $A^2\Pi_\Omega$ state of ClO (*ca.* 26 000 cm^{-1}, 311 kJ mol^{-1}). The formation of excited $^1\Delta$ oxygen is energetically allowed, however, it was excluded in a previous study of the reaction (1) [12]. Thus, all reaction products are formed in their electronic ground state, O_2 ($^3\Sigma_g^-$) and $ClO(^2\Pi)$.

A trajectory study [13] of the reaction (1) suggests that there is no evidence for a long-living transition complex and a non-statistical energy distribution can be expected. The most probable vibrational state should be $v = 1$, but levels up to $v = 8$ should be populated. The estimated energy distribution is predicted as follows: 58% of the excess energy of the reaction (1) should be found in the ClO radical (vibrational 20%, rotational 19% and translational 19%) and from the remaining 42% only 12% are released as internal energy of the oxygen (30% translational energy).

Although the kinetics of reaction (1) have been studied extensively, our knowledge concerning the reaction dynamics is rather poor. The reason for this lack of information are technical problems related to sensitive and fast detection techniques for nascent ClO from chemical reactions. The resonance enhanced multi photon ionization technique (REMPI) was used for the detection of ClO in the photodissociation of OClO. However, this technique

[a] e-mail: K.gericke@tu-bs.de

[b] *Present address*: Institut für Physikalische Chemie, Universität Göttingen, Tammannstrasse 6, 37077 Göttingen.

can hardly be used for detecting nascent ClO from reactions because of the required number densities.

Other detection techniques, like absorption measurements require usually high pressures and longer delay times, compared with the laser induced fluorescence technique (LIF), resulting in a vibrational and rotational relaxation of ClO.

There are only two investigations in order to determine the energy distribution of ClO from the reaction (1), performed by Norrish *et al.* [14,15], and most recently by Matsumi *et al.* [16]. In the flash lamp photolysis study of Norrish *et al.*, ClO was observed in the $v = 0$–5 states by absorption measurements, but the experimental conditions where insufficient for observing vibrationally unrelaxed products. Furthermore, the authors describe their results concerning the vibrational distribution as "not yet certain", because of the insensitivity of this technique. A breakthrough was achieved by the investigations of Matsumi *et al.* which was based on a LIF investigation of ClO by using the four-wave mixing technique for generating the required one-photon excitation wavelength. The nascent vibrational product state distribution is strongly inverted $(v = 0):(v = 1):(v = 2):(v = 3):(v = 4) = 0.8{:}1{:}1.3{:}2.4{:}2.9$. A surprisal analysis indicates a peak around $v = 8$ which was extrapolated from these lower vibrational state populations. They also performed measurements of the vibrational relaxation rate, however, the N_2 pressures were fairly low and the observed vibrational relaxation of ClO was essentially caused by OClO. Thus, only an upper limit of the ClO + N_2 relaxation rate was obtained.

The energy distribution is not only very important for understanding the dynamics of that reaction, but might also be of great interest, because vibrationally excited ClO reacts more rapidly with ozone, which may lead to a larger ozone loss compared with ground state ClO, as already pointed out by Vaida *et al.* [17] and Ravishankara *et al.* [18]. Furthermore, strongly vibrationally excited ClO may react with other atmospheric species. On energetic reasons, even a reaction with nitrogen becomes possible [19], if the energy of reaction (1) is released as ClO vibration:

$$\mathrm{ClO}^* + \mathrm{N_2} \rightarrow \mathrm{N_2O} + \mathrm{Cl}\ (\Delta_R H = +100.4\ \mathrm{kJ\ mol^{-1}}) \quad (3)$$

where the endothermicity refers to the ground states of the reactants.

In fact, the formation of N_2O was observed in a flash photolysis study of a mixture of OClO and N_2 at atmospheric pressure [20]. In this context, it is important to know the vibrational distribution and the rate constant for relaxation of vibrationally excited ClO in order to determine the relevance of vibrationally excited ClO on the chemistry of the atmosphere.

In this paper, we report not only the vibrational energy distribution of ClO formed up to $v = 6$ in reaction (1), but also the rotational, spin-orbit, and Λ-substrate distributions in order to elucidate the reaction dynamics. Furthermore, we performed an estimate of the relaxation rate of vibrationally excited ClO in collisions with N_2 by measuring the vibrational distribution of ClO at different collision numbers, represented by different N_2 pressures. The two photon LIF technique was used to obtain completely state resolved spectra of ClO [21]. Comparable experimental results agree with former investigations; however, due to our extended study, a different interpretation of the role of vibrationally excited ClO in the atmosphere has to be performed.

2 Experimental

Ozone was synthesized in a silent discharge from oxygen (Linde 4.0), adsorbed on silicagel at −110 °C and purified by a distillation at the temperature of liquid nitrogen. Chlorine (Matheson) and ozone were pumped directly into the stainless steel reaction chamber through separate effusive nozzles. The gas flow was controlled by glass valves. The cell pressure was determined at any time by a capacitance pressure gauge (Baratron). The two gases cannot be premixed before entering the reaction chamber, because the chain reaction, reactions (1) and (2), removes the ozone and no ClO is detectable, due to the presence of chlorine atoms in the gas system (*i.e.* by wall-collisions of chlorine).

The chlorine atoms were produced in the photolysis of Cl_2 near the maximum of the first UV-absorption spectrum. The radiation at 351 nm was delivered by a XeF excimer laser (Lambda 201 MSC) and slightly focused by a 50 cm quartz lens into the reaction chamber. The ratio of Cl_2:O_3 was 35 Pa:35 Pa. ClO was observed by the $2h\nu$-LIF technique [21]. The ClO was excited by a laser pulse delivered from a XeCl excimer laser (Lambda LPX 100) pumped dye laser (Lambda FL3000E). The spectrum in the 338–345 nm region (two photon excitation wavelength) was recorded with PTP (Radiant Dyes), the spectrum in the 345–365 nm region was recorded with RDC 360-neu (Radiant Dyes) as active laser medium, dissolved in dioxane. The typical output power was 10 mJ (PTP) and 14 mJ (RDC 360-neu) at a laser bandwidth of less than 0.4 $\mathrm{cm^{-1}}$. The laser output energy was monitored during the scans for normalizing the spectra to the laser intensity. The probe laser beam was focused by a 50 cm quartz lens into the reaction chamber, counter propagating to the photolysis laser beams. Fluorescence around 170 nm was observed with a CsI solar blind photomultiplier (EMR-542G-08-18) perpendicular to each laser beam. This photomultiplier is unable to detect light from both laser beams and, therefore, only VUV fluorescence light of ClO is detected, *i.e.* no scattered laser light is registered. This is important because of the short fluorescence lifetime of excited ClO, which is within the laser pulse length (< 20 ns), so that straylight signals cannot be removed by gating the detection time. The photomultiplier output was fed into a boxcar averager (Stanford Research Systems 250) and stored in a microcomputer (AT-386) after A/D conversion.

No fluorescence signal from ClO($v > 0$) is observed in absence of the photolysis laser beam or when the photolysis laser fires after the probe pulse. The signal also

vanishes when the ozone or chlorine gas flow is stopped. Thus, ClO($v > 0$) generated by reaction (1) is observed. In case of ClO($v = 0$) some signal remains when the photolysis laser is fired after the probe laser. The signal vanishes after about 10 laser shots (1 second) after interrupting the photolysis laser beam. The effect may result from ClO produced in former photolysis laser shots or from ClO, produced in a chain reaction (1) and (2). In order to suppress this effect, it is necessary to increase the gas flow, which leads to a strong consumption of ozone and chlorine. Since the higher vibrational levels are not affected, as described below and since ozone is only available in small amounts because of its synthesis, the ClO($v > 0$) is observed at lower flow rates. The delay between photolysis and detection laser pulse was 2.5 μs, determined by a fast photodiode which detected both the photolysis and the detection laser beam.

In order to study the influence of collisions on the vibrational distribution, ClO($C \leftarrow X$) spectra were measured by adding 500 Pa–10 000 Pa nitrogen to the reaction chamber. For these measurement the delay time between photolysis and detection was fixed at 3.5 μs.

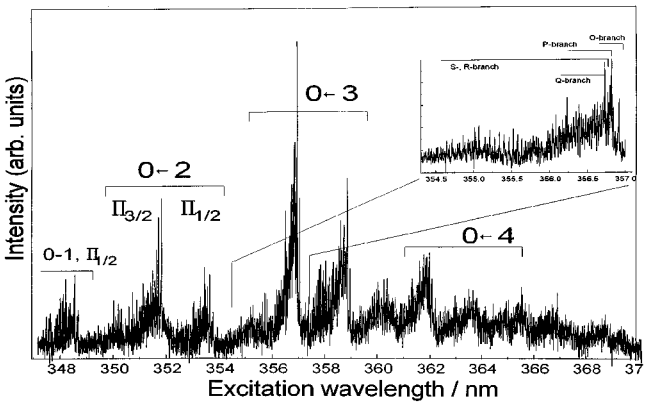

Fig. 1. Part of the $2h\nu$ LIF spectrum of ClO($C^2\Sigma,\ v' \leftarrow \Pi_\Omega,\ v$). The assignments of the observed band systems are carried out by fitting procedures. Each band system contains the transitions from the $\Pi_{1/2,\ 3/2}$ ground state of ClO. The inset in the upper right corner shows the rotational fine structure of ClO($C^2\Sigma,\ v' = 0 \leftarrow \Pi_\Omega,\ v = 3$). This spectrum was recorded with a delay time of 200 ns, at a collision number of *ca.* 2.

3 Results and discussion

The 351 nm photolysis of Cl_2 produces Cl atoms almost exclusively in the energetically lowest spin-orbit-state, $^2P_{3/2}$ [22]. In the centre of mass system the mean collision energy is given by

$$E_{coll} = \frac{1}{2}\mu(v_{\mathrm{Cl}}^2 + v_{\mathrm{O_3}}^2 + v_{\mathrm{Cl_2}}^2)$$

where μ is the reduced mass of the Cl+O_3 system and $v_{\mathrm{O_3}}$ and $v_{\mathrm{Cl_2}}$ are calculated according to

$$v = \sqrt{\frac{3RT}{m}}\,.$$

The velocity of the chlorine atom v_{Cl} is determined *via* the translational energy of the Cl atom, $E_{trans}(\mathrm{Cl}) = (E_{h\nu}(351\ \mathrm{nm}) - D_0(\mathrm{Cl–Cl}))/2$. A value of $E_{coll} = 26$ kJ/mol is obtained for the mean collision energy. In some experiments nitrogen was added, leading to a thermalization of the initially hot chlorine atoms. In that case, the collision energy is $E_{coll} = 3.7$ kJ/mol. The available energy E_{av}, composed of the exothermicity of reaction (1), $\Delta_R H = -162.6$ kJ/mol, and the collision energy of the Cl atoms (nascent conditions), allows population of the ClO vibrational levels up to $v = 20$.

The observed ClO LIF spectrum in the region between 350 nm and 362.5 nm resulting from the reaction of Cl with O_3 is shown in Figure 1. The assignments were performed by fitting a theoretical spectrum to the observed data [21]. All fluorescence signals were normalized with respect to the laser intensity.

The spin-orbit state population was determined by integrating the band system ($\Pi_{3/2}$ or $\Pi_{1/2}$) of each vibrational transition. The ratios of the spin orbit state population $R(v) = P(\Pi_{3/2})/P(\Pi_{1/2})$ in different vibrational states are listed in Table 1. The obtained population of the spin orbit states $R(v > 0)$ for vibrationally excited states ($v > 0$) is found to be (1.5 ± 0.25):1. This ratio is far from the thermal equilibrium at 298 K where $R(298\ \mathrm{K}) = 4.7$:1, calculated from a Boltzmann distribution which agrees with measurements of a completely relaxed spectrum [21]. The population of the $\Pi_{3/2}$ to $\Pi_{1/2}$ system for the nascent distribution would correspond to a temperature of 1100 K. An exception of this (1.5:1) ratio is the distribution of the $v = 0$ spin orbit states. The ratio of $R(v = 0) = 3$:1 indicates the presence of relaxed ClO. If one assumes that the spin-orbit state distribution in $v = 0$ is the same as in higher vibrational states, than one can calculate the amount of relaxed (r) and nascent (n) ClO:

$$rR(298\ \mathrm{K}) + nR(nascent) = R(v = 0,\ observed) = 3$$

$$r = 0.47$$

where the experimental values $R(v = 0,\ 298\ \mathrm{K}) = 4.7$ and $R(v = 0,\ nascent) = 1.5$, and the conservation law, $r + n = 1$, have been used. Thus, almost 50% of ClO ($v = 0$) may result from other sources than reaction (1).

The assignments of the transitions and the population are also given in Table 1. It is important to mention that only transitions belonging to $(v' = 0, 1) \leftarrow (v = 0$–$6)$ were observed, due to a predissociation of the ClO($C^2\Sigma$) electronic state, as already assumed by Matsumi *et al.* [23]. The population of the vibrational levels were determined by integration of the observed intensity of each vibrational transition. The Franck-Condon factors for the transitions belonging to the $v' = 0 \leftarrow v > 4$ transitions are very small [24], and therefore, observation of ClO is limited within moderate error limits (15%) to the $v = 4$ state. The transitions belonging to $v' = 1 \leftarrow v = 0$–6 are weak, compared to the transitions belonging to $v' = 0 \leftarrow v = 0$–4, although the Franck-Condon factors are similar. From the intensity ratio of the $(v' = 0 \leftarrow v = 3)$:$(v' = 1 \leftarrow v = 3)$

Table 1. Franck-Condon factors, populations and spin-orbit ratios of the observed vibrational transitions from ClO in the reaction of O_3 with Cl.

$v' \leftarrow v$	FC^a	Position / nm^b	$P(v)_{exp}$/ %^{c}	$P(v)_{Prior}$/ %	$P(\Pi_{3/2}) : P(\Pi_{1/2})$
$0 \leftarrow 0$	0.3107	341.73 (343.61)	7 ± 1	21	3.02
$0 \leftarrow 1$	0.3412	346.72 (348.65)	4 ± 1	17	1.66
$0 \leftarrow 2$	0.2074	351.81 (353.77)	9 ± 1	11	1.42
$0 \leftarrow 3$	0.0924	356.96 (358.97)	31 ± 3	9	1.28
$1 \leftarrow 3$	0.2013	350.30			
$0 \leftarrow 4$	0.0336	362.21 (363.78)	27 ± 3	7	1.41
$1 \leftarrow 4$	0.1635	355.09			
$0 \leftarrow 5$	0.0106	366.73 (368.63)	14 ± 7	5	1.22
$1 \leftarrow 5$	0.1635	360.47			
$1 \leftarrow 6$	0.0377	365.41	8 ± 4	4	

[a] From reference [23].
[b] Band head of the P-branch of the $\Pi_{3/2}(\Pi_{1/2})$ system.
[c] Some values for $1 \leftarrow x$ cannot be given, since some transitions are not observed or interfere with $0 \leftarrow x$ transitions.

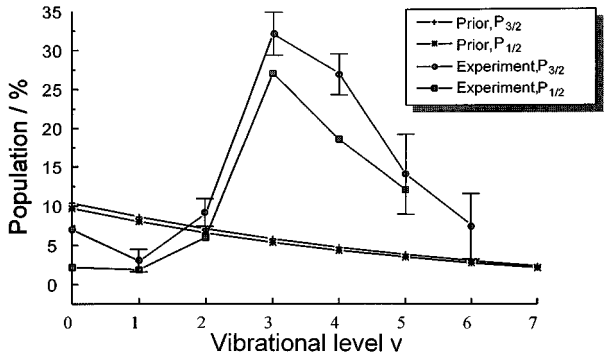

Fig. 2. Vibrational energy distribution of ClO, formed in the reaction of chlorine with ozone, compared to a prior distribution. The population of the vibrational levels reaches a maximum at $v = 3$.

and the $(v' = 0 \leftarrow v = 4)$:$(v' = 1 \leftarrow v = 4)$ transitions and the respective Franck-Condon factors we calculate that 80% of ClO($C^2\Sigma$, $v' = 1$) predissociates within the fluorescence lifetime (> 20 ns). The transitions into $v' = 1$ were used to determine the ClO vibrational state population above $v = 4$. Due to predissociation there is a larger uncertainty in the determination of the product state population of $v = 5$ and $v = 6$ (25%).

The vibrational state distribution of ClO is shown in Figure 2. It exhibits a maximum around $v = 3$ and $v = 4$. The distribution implies that a certain amount of ClO in the lowest state, $v = 0$, originates from a different source, which was already expected from the spin orbit state distribution. It is important to mention that under the experimental conditions listed above (~ 15 gas kinetic collisions) the vibrational distribution is not affected by subsequent relaxation processes. This can be concluded not only from the results of Matsumi *et al.* [16] but also from measurements discussed below, where nitrogen was added as collision partner. A significant change of the observed vibrational distribution was found only for much higher collision numbers.

Contrary to the results of the trajectory study which predicts a peak at $v = 0$, ClO is generated mainly in higher vibrational states, but compared with the possible vibrational excitation of $v = 20$ on purely energetic considerations, the vibrational excitation is moderate. Because of the limitations listed above, we could not observe vibrational states for $v \geq 7$. However, there is an increase of the vibrational state population up to $v = 3$–4 followed by a strong decrease to $v = 6$. Although it cannot completely be ruled out, it seems to be unlikely that the vibrational distribution again increases at higher v. Therefore, we assume that nearly all ClO(v) products are observed in the present experiment and that Figure 2 represents the complete vibrational state distribution of ClO formed in the reaction of Cl+O_3. Under this assumption the fraction of E_{av} found as vibrational energy is $f_{vib} = 16\%$. The obtained vibrational state distribution of ClO seems to be slightly different from the observations of Matsumi *et al.* [16] who found a maximum of the vibrational distributing at $v = 4$, very close to the highest observed state ($v = 5$). However, taking into account the error limits of both investigations, there is no remarkable difference in the observed ClO($v = 0$–5) distributions.

In order to determine the rotational distribution, the ClO($C^2\Sigma, v = 0$) $\leftarrow$ ClO($X^2\Pi, v = 3$) transition (Fig. 1) was recorded with a 200 ns delay between photolysis and detection laser pulses at a cell pressure of 7 Pa ozone and 7 Pa chlorine. The populations of the rotational levels were obtained by fitting the simulated spectrum to the measured spectrum by a least-square fitting procedure as described in an earlier paper [21]. Under the experimental conditions (~ 2.4 gas kinetic collisions), only the lower rotational states are relaxed as shown in the Boltzmann plot in Figure 3. The rotational temperature is approximately (1300 ± 200) K (high J). The measured population ratio of the spin orbit states R $(v = 3) = 1.3{:}1$ corresponds to the observed spin-orbit state population ratio at higher

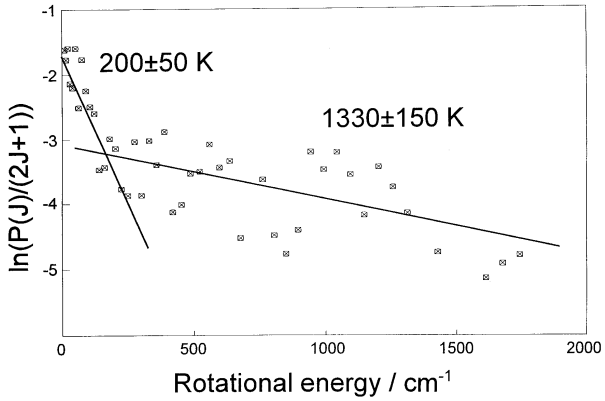

Fig. 3. The vibrational distribution of the $v = 3$ vibrational state of ClO, obtained from the spectrum shown in the upper right corner of Figure 1, represented as a "Boltzmann plot". The rotational distribution at higher rotations can be described by a temperature of 1300 K. The lower rotational levels show a significant lower rotational temperature, 200 K, which is probably caused by relaxation processes.

collision numbers (Tab. 1). If we assume that the rotational temperature obtained from higher J represents the nascent rotational temperature in each vibrational level, then $\langle E_{rot} \rangle = 900$ cm^{-1} is released as mean rotational energy of ClO, corresponding to 6% of the available energy E_{av}.

No specific preferred population of a Λ-doublet state was observed. Measurements of the linewidth in order to obtain the kinetic energy of the ClO fragment were not possible, because such experiments require completely collision free conditions, which could not be guaranteed for the required signal intensities.

In summary, we observed a strongly inverted population of the vibrational levels and a moderate rotational excitation of the ClO fragment. For modeling the reaction mechanism, we performed a statistical analysis of the expected ClO energy distribution (prior distribution). By using the standard equations to determine this prior distribution of a four atomic system $A + BCD \rightarrow AB + CD$

$$P^{\circ}(V_{AB}, V_{CD}, J_{AB}, J_{CD}) \propto (2J_{AB} + 1)(2J_{CD} + 1) \times \sqrt{E_{av} - E_v(AB) - E_{rot}(AB) - E_v(CD) - E_{rot}(CD)}$$

$$P^{\circ}(V_{AB}, J_{AB}) = \sum_{V_{CD}, J_{CD}} P^{\circ}(V_{AB}, V_{CD}, J_{AB}, J_{CD}).$$

We calculate the statistical energy distribution of the ClO(AB) fragment. By comparing the experimental vibrational distribution with the prior distribution (Fig. 2), the significant difference between both distributions becomes obvious. The measured lower vibrational levels are much less populated, compared with the predictions of the prior distribution. Therefore, the reaction proceeds non-statistically, and there is no evidence for a long-living transition complex, which would favour a statistical energy distribution. Only 22% of the available energy is found as internal energy of the ClO fragment. Most of the energy should be released as translational energy or as internal energy of O_2. This observation does not agree with the trajectory study, which predicts that an equal amount of E_{av} is found in each degree of freedom of ClO.

An inspection of the potential energy surface (LEPS) of the ClO_3 transition complex using the equations of reference [13] shows two principal reaction paths:

1. the chlorine atom approaches along a line containing an oxygen-oxygen bond (Fig. 6);
2. the chlorine atom approaches perpendicularly to the ozone plane, resulting in a nearly D_{3h} symmetry for the transition complex (Fig. 7).

The potential energy surface for the D_{3h} transition complex shows a minimum of the potential energy of −7.1 eV, which can only be reached via a high barrier of 4 eV. The energy of the reactants in our experiment is insufficient to pass this barrier. Even if this barrier could be passed, the LEPS potential of this geometry indicates a long-living transition complex. Thus, we assume that the reaction of Cl+O_3 takes place in a plane, where the chlorine atom attacks the ozone molecule essentially along an oxygen bond (Fig. 6). First results of *ab initio* calculations also indicate a planar reaction geometry [25]. However, the minimum of the potential energy is not exactly in the direction of an O–O bond, but deviates slightly from such a "linear" geometry.

It is important to know the vibrational relaxation rate of ClO because of the possible reactions of strongly vibrationally excited ClO with other species present in the lower stratosphere. Calculations of the reaction probability depend on the number of collisions where ClO has sufficient internal energy to react. Vibrationally excited ClO is not only produced in the present reaction under study, but also in the photolysis of OClO [26], which is an important source of ClO in the atmosphere. Some recorded ClO spectra in the Cl+O_3 system are shown in Figure 4, where N_2 as major ClO collision partner has been added. The extracted ClO vibrational state distributions of these relaxation measurements are shown in Figure 5. There is a significant change of the maximum of the distribution from $v = 3$–4 (nascent distribution) to $v = 2$–3 (10 000 Pa nitrogen added, ∼ 2700 gas kinetic collisions).

The observed vibrational distributions under various nitrogen cell pressures were compared with an analytical solution of rate equations which describe the vibrational relaxation of the ClO. Starting with the nascent distribution, we assume a relaxation of ClO of first order from each vibrational level to the next lower one, using the same relaxation rate constant for each step. Although this is a crude model for the vibrational relaxation, the obtained k value should be accurate within one order of magnitude and, thus, the significance of atmospheric reactions of vibrationally excited ClO can be estimated.

The highest populated level, $v = 6$, will have the index $i = 1$ and can only be depopulated due to collisions in

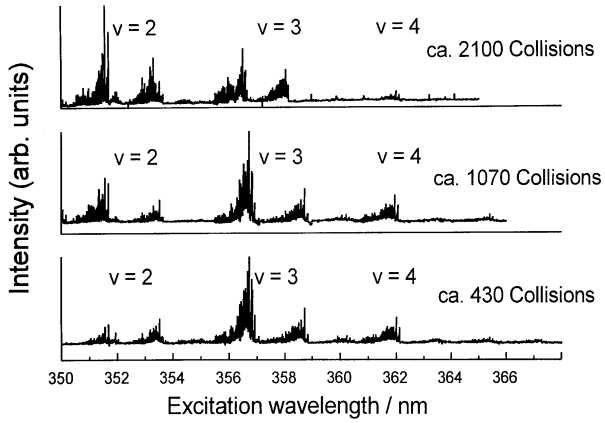

Fig. 4. Change of the ClO-LIF spectrum as a function of collision numbers. The population of higher vibrational levels decreases, whereas the population of lower vibrational levels increases.

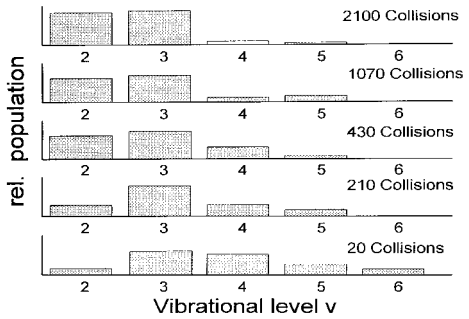

Fig. 5. Relative populations of the vibrational levels of ClO after collisions with nitrogen.

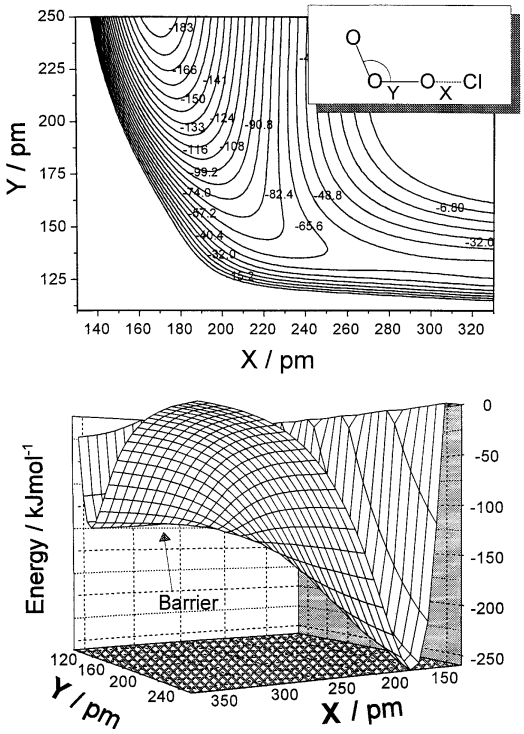

Fig. 6. Potential energy surface (LEPS) of the transition complex ClO_3, using the equations of reference [13], assuming that the chlorine atom approaches along an oxygen-oxygen bond. The numbers show the relative energy in kJ/mol. There is no substantial barrier (1.4 kJ/mol), which may explain the non-statistical distribution of ClO as product of this reaction.

favour of the next lower level $v = 5$ ($i = 2$):

$$\mathrm{ClO}(v = 6) + \mathrm{M} \rightarrow \mathrm{ClO}(v = 5) + \mathrm{M}^*.$$

That level ($i = 2$) will be depopulated in favour of the next lower one ($i = 3$), *etc.*:

$$\begin{aligned} N_1 &= N_{1,0}e^{-kt} \\ N_2 &= -kN_2 + kN_{1,0}e^{-kt} \\ N_3 &= -kN_3 + k(ktN_{1,0} + N_{2,0})e^{-kt} \\ &\textit{etc.} \end{aligned}$$

where $N_{i,0}$ is the nascent vibrational population of the level i. Combining the solutions of the equations for the six (within one scan) observed vibrational levels $N_1 - N_6$ leads to the simple expression

$$N_i(t) = e^{-kt}\left(\sum_{j=1}^{i}\frac{(kt)^{j-1}}{(j-1)!}N_{i-j+1,0}\right).$$

In the experiment we did not increase the delay time in order to increase the collision numbers, because we wanted to prevent flyout of the ClO from the detection volume. Instead, the cell pressure was varied and the calculated collision frequencies were converted into a delay time at a pressure of 70 Pa (value for the nascent spectrum). The populations of the vibrational levels of each spectrum were obtained by integration of the vibrational transition in the same manner as the values of the nascent ClO. A value of $k = 2 \times 10^{-13}$ cm^{3}molecule^{-1}s^{-1} gives the best results compared with the experimental data. A variation of k by a factor of two shows already some remarkable difference to the experimental distributions. It should be mentioned that this value is obtained mainly by collisions of ClO with N_2 and not by relaxation processes induced by Cl or O_3.

The highest ozone concentration in the atmosphere of 10^{13} molecule cm^{-3} is at an altitude around 25 km. The total concentration of nitrogen and oxygen is about 10^{18} molecule^{-1}cm^3 at this altitude. Thus, a ClO molecule will collide roughly 10^5 times more often with N_2 (or O_2) than with ozone. From these concentrations and the value of k, one calculates that more than 99% of the ClO are transferred into the vibrational ground state before a collision with an ozone molecule takes place. Thus, vibrationally excited ClO will not survive under stratospheric conditions. As a consequence, the influence of vibrationally excited ClO on the ozone destruction cycle, as assumed by Vaida *et al.* [17], can be neglected. However, a reaction of highly vibrationally excited ClO with nitrogen is still possible, provided the ClO internal energy balances

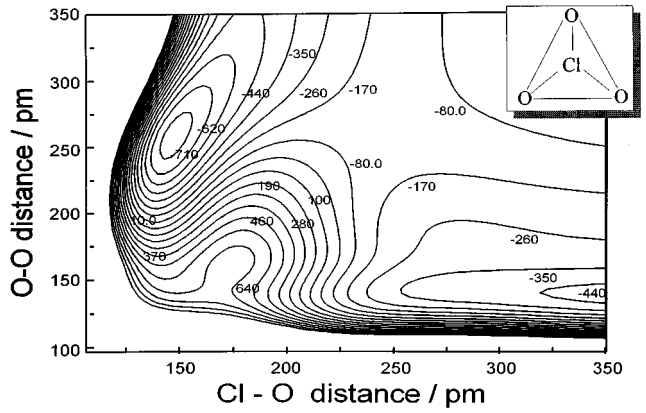

Fig. 7. Potential surface of the ClO_3 transition complex, calculated if the chlorine atom approaches perpendicularly to the ozone plain (C_{3v}-symmetry). There is a high barrier of about 400 kJ/mol and a minimum of ClO_3 (D_{3h}-symmetry) of about 300 kJ/mol. This minimum should lead to a more statistical energy distribution.

the required energy for such process, because several thousand encounters take place before the internal ClO energy is below the energetic threshold for the reaction. Indeed, observations of highly vibrationally excited ClO [26] and final product analysis support the assumption of Cl and N_2O production in the reaction of $ClO(v \gg 0) + N_2$ [20].

In summary, we have shown that ClO as a product of a chemical reaction can be observed by the two photon LIF technique. ClO is formed in the important atmospheric reaction Cl+O_3 with high vibrational excitation and moderate rotational excitation. The reaction geometry is planar and a long living intermediate seems to be unlikely. The vibrational relaxation by collisions with nitrogen is fast compared to the reaction of vibrationally excited ClO with ozone under stratospheric conditions. Therefore, reactions of vibrationally excited ClO with atmospheric trace components can be ruled out.

Support by the Deutsche Forschungsgemeinschaft is gratefully acknowledged. We thank Professors F.J. Comes and E.A. Reinsch for helpful discussions. SB thanks the Konrad-Adenauer-Stiftung for fellowship support.

References

1. R.S. Stolarski, R.J. Cicerone, Can. J. Chem. **52**, 1620 (1974).
2. M.J. Molina, L.T. Molina, J. Phys. Chem. **91**, 433 (1987).
3. M.J. Prather, R.T. Watson, Nature **344**, 729 (1990).
4. J.G. Anderson, D.W. Toothey, W.H. Brune, Science **251**, 29 (1991).
5. W.H. Brune, J.G. Andersen, D.W. Toothey, D.W. Fahey, S.R. Kawa, R.L. Jones, D.S. McKenna, L.R. Poole, Science **252**, 1260 (1991).
6. S. Salomon, Nature **347**, 347 (1990).
7. J.M. Nicovich, K.D. Kreutter, P.H. Willis, Int. J. Chem. Kinet. **22**, 399 (1990).
8. R.T. Watson, G. Machado, S. Fischer, D.D. Davis, J. Chem. Phys. **65**, 2126 (1976).
9. M.S. Zahniser, F. Kaufmann, J.G. Anderson, Chem. Phys. Lett. **37**, 226 (1976).
10. M.J. Kuryolo, W. Braun, Chem. Phys. Lett. **37**, 232 (1976).
11. Atkinson, J. Phys. Chem. Ref. Data **21**, 1410 (1992).
12. K.Y. Choo, M.T. Leu, J. Chem. Phys. **89**, 4832 (1985).
13. S.C. Farantos, J.N. Murrell, Int. J. Quant. Chem. **XIV**, 659 (1978).
14. F.H.C. Lipscomp, R.G.W. Norrish, Proc. Roy. Soc. Lond. A. **233**, 455 (1956).
15. W.D. McGrath, R.G.W. Norrish, Z. Phys. Chem. **15**, 245 (1958).
16. Y. Matsumi, S. Nomura, M. Kawasaki, T. Imamura, J. Phys. Chem. **100**, 176 (1996).
17. V. Vaida, E.C. Richard, A. Jefferson, L.A. Cooper, R. Flesch, E. Rühl, Ber. Bunsenges. Phys. Chem. **96**, 391 (1992).
18. J. M. Nicovich, P.H. Wine, A.R. Ravishankara, J. Chem. Phys. **89**, 5670 (1988).
19. F. Kaufmann, N.J. Gerri, D.A. Pascale, J. Chem. Phys. **24**, 32 (1956).
20. R.F. Delmdahl, K.H. Gericke, Chem. Phys. Lett. **281**, 407 (1997).
21. S. Baumgärtel, K.-H. Gericke, Chem. Phys. Lett. **227**, 461 (1994).
22. G.E. Busch, R.T. Mahoney, R.I. Morse, K.R. Wilson, J. Chem. Phys. **51**, 449 (1969).
23. Y. Matsumi, S.M. Shamsuddin, M. Kawasaki, J. Chem. Phys. **101**, 8262 (1994).
24. J.B. Nee, K.J. Hsu, J. Photobiol. A **55**, 269 (1991).
25. M. Wagner, E.A. Reinsch, K.-H.Gericke (to be published).
26. M. Roth, C. Maul, K.-H. Gericke, J. Chem. Phys. **107**, 10582 (1997).